THE JOURNAL OF BIOLOGICAL CHEMISTRY VOL. 284, NO. 26, pp. 17438–17448, June 26, 2009

Host Cell P-glycoprotein Is Essential for Cholesterol Uptake and Replication of *Toxoplasma gondii*[*][S]

Received for publication, December 15, 2008, and in revised form, March 27, 2009 Published, JBC Papers in Press, April 22, 2009, DOI 10.1074/jbc.M809420200

Iveta Bottova[‡], Adrian B. Hehl[‡], Saša Štefanić[‡], Gemma Fabriàs[§], Josefina Casas[§], Elisabeth Schraner[¶], Jean Pieters[‖], and Sabrina Sonda[‡1]

From the Institutes of [‡]Parasitology and [¶]Veterinary Anatomy, University of Zurich, 8057 Zurich, Switzerland, the [§]Institut de Química Avançada de Catalunya, Consejo Superior de Investigaciones Científicas, 08034 Barcelona, Spain, and [‖]Biozentrum, University of Basel, 4056 Basel, Switzerland

P-glycoprotein (P-gp) is a membrane-bound efflux pump that actively exports a wide range of compounds from the cell and is associated with the phenomenon of multidrug resistance. However, the role of P-gp in normal physiological processes remains elusive. Using P-gp-deficient fibroblasts, we showed that P-gp was critical for the replication of the intracellular parasite *Toxoplasma gondii* but was not involved in invasion of host cells by the parasite. Importantly, we found that the protein participated in the transport of host-derived cholesterol to the intracellular parasite. *T. gondii* replication in P-gp-deficient host cells not only resulted in reduced cholesterol content in the parasite but also altered its sphingolipid metabolism. In addition, we found that different levels of P-gp expression modified the cholesterol metabolism in uninfected fibroblasts. Collectively our findings reveal a key and previously undocumented role of P-gp in host-parasite interaction and suggest a physiological role for P-gp in cholesterol trafficking in mammalian cells.

P-glycoprotein (P-gp, ABCB1, MDR1)[2] is one of the most intensively studied members of the ABC transporter superfamily. With remarkably broad substrate recognition, P-gp drives the ATP-dependent efflux of toxic metabolites and xenobiotics from the cell (1) and is thus a central mediator of drug bioavailability. Importantly, P-gp overexpression following drug treatment is responsible for the multidrug resistance (MDR) phenotype, a major reason for chemotherapy failure not only in cancer cells (2) but also in pathogenic microorganisms (3, 4). Aside from its well known role in drug efflux, P-gp is also expressed at basal levels in many different tissues, yet the normal physiological functions of the protein remain poorly understood.

The possibility that physiological levels of host P-gp play a role in host-pathogen interaction, other than mediating drug resistance, has not been investigated so far. We addressed this question using *Toxoplasma gondii* as a model pathogenic parasite. *T. gondii* is the causative agent of toxoplasmosis, a potentially fatal disease not only for immunocompromised patients and fetuses but according to recent insights also emerging as a life threatening infection in immunocompetent individuals (5). *T. gondii* infects virtually all nucleated host cells and resides in a highly specialized vacuole, called the parasitophorous vacuole (PV), which is formed by invaginating the host cell membrane at the time of invasion. The PV is not competent for lysosome fusion, thus avoiding acidification (6), but it is closely associated with host organelles, including lysosomes, mitochondria, and endoplasmic reticulum (reviewed in Ref. 7). Even though the PV does not intersect directly with host vesicular traffic, *T. gondii* remains dependent on host cells for a number of critical nutrients. Significant progress has been made in our understanding of the mechanisms *T. gondii* uses to scavenge nutrients from its host, especially in the case of lipid molecules. An important recent example was the identification of H.O.S.T. (host organelle-sequestering tubulo-structures), a unique system of tubular structures formed by the parasite to sequester cholesterol-containing endolysosomes from the host cytoplasm into the PV (8). However, the molecular mechanisms of the traffic from the host cell to the PV are not completely elucidated, and the existence of transporters has been proposed frequently.

To analyze whether the P-gp transporter plays a role in *T. gondii* biology we compared parasite replication in wild type (WT) mouse embryonic fibroblasts with double knock-out (DKO) fibroblasts in which neither of the two murine P-gp isoforms are expressed (9). In parallel, we also analyzed DKO cells complemented with the human P-gp homologue (DKO/P-gp) (10), which restored P-gp functionality to DKO cells and allowed P-gp expression levels higher than those found in WT cells (supplemental Fig. S1). In this way, our model did not depend on either drug-selected P-gp-overexpressing cells, which may acquire adaptation mechanisms different from P-gp overexpression during the development of the MDR phenotype, or P-gp inhibitors, several of which are known to have side effects on host metabolism.

EXPERIMENTAL PROCEDURES

Biochemical Reagents—Unless otherwise stated, all chemicals were purchased from Sigma, cell culture reagents were

* This work was supported by grants from the Marie Heim-Vögtlin Foundation, Fondation Pierre Mercier pour la Science, Roche and Novartis (to S. S.), Bundesamt für Bildung and Wissenschaft C03.0007 COST Action 857 (to A. B. H.), and the Swiss National Foundation (to J. P.).

[S] The on-line version of this article (available at http://www.jbc.org) contains supplemental Figs. S1–S6.

[1] To whom correspondence should be addressed: Institute of Parasitology, University of Zurich, Winterthurerstrasse 266a, 8057 Zurich, Switzerland. Tel.: 41-44-6358514; Fax: 41-44-6358907; E-mail: sabrina.sonda@vetparas.uzh.ch.

[2] The abbreviations used are: P-gp, P-glycoprotein; MDR, multidrug resistance; PV, parasitophorous vacuole; WT, wild type; DKO, double knock-out; PBS, phosphate-buffered saline; CD, methyl-β-cyclodextrin; HDL, high density lipoprotein(s); p.i., post-infection; H.O.S.T., host organelle-sequestering tubulo-structures; apoA-I, apolipoprotein A-I.

from Invitrogen, and radiolabeled lipids were from Amersham Biosciences. Anti-P-gp monoclonal antibody C219 was purchased from Alexis Biochemicals; anti-Lamp1 1D4B antibody was obtained through the Developmental Studies Hybridoma Bank (University of Iowa, Iowa City, IA); anti-giantin and anti-tubulin were a kind gift from J. Rohrer and M. A. Hakimi, respectively. Conjugated secondary antibodies were from Invitrogen. Reconstituted high density lipoproteins and apolipoprotein A-I (apoA-I) were a kind gift from P. Lerch (CSL Behring, Bern, Switzerland). NDB-cholesterol was from Avanti Polar Lipids.

Mammalian Cell and Parasite Culture—Mouse embryonic fibroblasts double knocked out for P-gp (77.1, Mdr1a$^{-/-}$/Mdr1b$^{-/-}$) (9), triple knocked out for P-gp and MRP1 (3.8, Mdr1a$^{-/-}$/Mdr1b$^{-/-}$/Mrp1$^{-/-}$) (11) and parental cells were kindly provided by A. Schinkel (The Netherlands Cancer Institute, Amsterdam, The Netherlands). Mdr1 transfected 77.1 (10) and G185 NIH 3T3 fibroblasts (12) were a generous gift from M. M. Gottesman (National Cancer Institute, National Institutes of Health, Bethesda, MD).

The cells were routinely cultured in Dulbecco's modified Eagle's medium supplemented with 10% fetal calf serum, 2 mM glutamine, 50 units of penicillin/ml, and 50 μg of streptomycin/ml at 37 °C with 5% CO_2. Mdr1 transfected 77.1 and G185 cells were maintained in 20 and 60 ng/ml colchicine, respectively. Colchicine was removed from the culture medium during parasite infection.

β-Galactosidase expressing *T. gondii* and *Neospora caninum* were a kind gift from J. Boothroyd and D. Sibley, respectively. The parasites were maintained by serial passages in mouse embryonic fibroblasts, harvested from infected host cells by passage through a 26-gauge needle, and purified by separation on Sephadex-G25 columns (Amersham Biosciences) as described (13). Purified parasites were counted in a hemocytometer chamber and used for a new cycle of host cell invasion at the multiplicity of infection of 1. Parasite burden was quantified after 24 h by direct parasite counting or after 48 or 72 h by colorimetric detection of parasite β-galactosidase using chlorophenol red-β-D-galactopyranoside as substrate, as described (14). In some experiments, parasite quantification in infected host cells was performed by flow cytometry analysis on a FACSCalibur flow cytometer (Becton Dickinson), after staining permeabilized cells with a rabbit polyclonal anti-*T. gondii* tachyzoite antiserum (15) at 1:2000 dilution, followed by fluorescein-conjugated anti-rabbit secondary antibody at 1:300 dilution. Parasite invasion was determined by dual color immunostaining with the described anti-*T. gondii* antiserum to differentiate intracellular and extracellular parasites, as described (16).

Lipid Analyses—For cholesterol transport to intracellular *T. gondii*, infected host cells were labeled with 0.5 μCi/ml [^{3}H]cholesterol for 5 h. After extensive washing with PBS and 0.05% fat-free bovine serum albumin in PBS, parasites were isolated as previously described and counted, and the associated radioactivity was measured by liquid scintillation. Background radioactivity resulting from host cell debris was determined using similarly processed uninfected host cells and subtracted from parasite samples.

For cholesterol uptake analysis, host cells were incubated with 0.5 μCi/ml [^{3}H]cholesterol for 5 h and extensively washed, and cell-associated radioactivity was measured by liquid scintillation. Steady state cholesterol mass was assessed using the Amplex Red kit (Invitrogen) or by lipid extraction according to Bligh and Dyer (17) and high performance thin layer chromatography separation of aliquots corresponding to equal protein content on Silica Gel 60 plates in benzene/2-propanol/water (100:10:0.25). The bands were visualized with 10% $CuSO_4$ in 8% aqueous phosphoric acid and quantified by densitometry.

Liquid chromatography-mass spectrometry analysis of lipids from *T. gondii* grown in WT or DKO host cells was performed as described (18) in a Waters Aquity UPLC system connected to a Waters LCT Premier orthogonal accelerated time of flight mass spectrometer (Waters, Millford, MA), operated in positive electrospray ionization mode.

For analysis of sphingolipid synthesis in *T. gondii*, purified parasites were labeled with 0.5 μCi/ml [^{3}H]palmitic acid for 3 h, lipids were extracted as before and aliquots corresponding to equal protein content were separated by high performance thin layer chromatography using chloroform/methanol/25% NH_4OH (65:25:4.5). Radiolabeled bands were visualized by use of a tritium-sensitive screen (PerkinElmer Life Sciences) in a Personal Molecular PhosphoImager FX (Bio-Rad), identified according to co-migrating standards visualized by iodine vapors and quantified using ImageQuant software (Amersham Biosciences).

For kinetic of cholesterol esterification, host cells were labeled with 0.5 μCi/ml [^{3}H]cholesterol for 5, 24, and 48 h, and lipids were extracted as before and separated by high performance thin layer chromatography using benzene/2-propanol/water (100:10:0.25) as a solvent system. After iodine vapor visualization, bands co-migrating with cholesterol and cholesteryl ester standards were cut out of the plates, and the associated radioactivity was measured by liquid scintillation. The data for cholesterol esterification are reported as a percentage of [^{3}H]cholesteryl esters from total cellular [^{3}H]cholesterol.

For cholesterol extraction with methyl-β-cyclodextrin (CD) and efflux to reconstituted high density lipoproteins (HDL) or apoA-I, the cells were labeled with 0.5 μCi/ml [^{3}H]cholesterol for 24 h, extensively washed, and incubated with 2 mM CD, 20 μg/ml reconstituted HDL, or 10 μg/ml apoA-I in medium without fetal calf serum. Medium aliquots were measured by liquid scintillation at the time points indicated in the figures. Residual cell radioactivity was measured after cell solubilization in 0.1 N NaOH. Total radioactivity was calculated as medium + cell-associated radioactivity. Background efflux to medium alone was measured at the same time points and subtracted from the values obtained with the cholesterol acceptors CD, reconstituted HDL, and apoA-I.

Cholesterol Visualization and Immunofluorescence Analysis—To visualize intracellular transport of fluorescent cholesterol, host cells were seeded on glass slides and infected with *T. gondii* for 24 h. The cells were incubated with 5 μM NBD-cholesterol in Dulbecco's modified Eagle's medium without fetal calf serum for 1 h at 37 °C, fixed in 3% formaldehyde, mounted in Vectashield antifade agent (Vector Laboratories, Inc., Burlingame, CA), and imaged employing an excitation filter of 450–500 nm.

For visualization of unesterified cholesterol, the cells were seeded as before, fixed, and incubated with 0.05 mg/ml filipin in PBS, 10% fetal calf serum for 1 h at room temperature. The images were collected using an excitation filter of 350–410 nm. For visualization of esterified cholesterol in intracellular lipid droplets, the cells were fixed with 3% formaldehyde, blocked, and stained with Nile red at a concentration of 0.5 μg/ml in PBS for 20 min. The cells were extensively washed in PBS and mounted, and lipid fluorescence was analyzed employing an excitation filter of 450–500 nm.

For P-gp localization, DKO/Pgp host cells grown on glass slides were infected with *T. gondii* for 24 h, prior to fixation in acetone at −20 °C for 10 min. Anti-P-gp monoclonal antibody C219 was used at 1:10 dilution according to the manufacturer's instruction, followed by fluorescein-conjugated secondary antibody at 1: 200 dilution. *T. gondii* was stained with a rabbit polyclonal anti-*T. gondii* tachyzoite antiserum (15) at 1:2000 dilution, followed by Texas Red-conjugated anti-rabbit secondary antibody at 1:300 dilution. The nuclei were visualized with 4′,6-diamidino-2-phenylindole.

For endo-lysosome localization, host cells grown on glass slides were infected with *T. gondii* or *N. caninum* for 24 h, incubated with 6 μg/ml fluorescein-conjugated cholera toxin B subunit for 60 min at 37 °C, and analyzed after fixation. For lysosome and Golgi localization, cells were seeded as before, fixed, and stained with anti-Lamp1 (1:50) or anti-giantin (1:750) antibodies followed by fluorescein-conjugated secondary antibody.

Microscopy analyses were performed on a Leica DM IRBE fluorescence microscope or on a Leica SP2 AOBS confocal laser-scanning microscope (Leica Microsystems, Wetzlar, Germany), using the appropriate settings. Image stacks of optical sections were further processed using the Huygens deconvolution software package version 2.7 (Scientific Volume Imaging, Hilversum, NL).

Transmission Electron Microscopy Analysis—Host cells grown on sapphire disks were infected with *T. gondii* and incubated at 37 °C for 24 h, prior to fixation with 0.25% glutaraldehyde and freezing in a high pressure freezing machine (HPM 010, BAL-TEC) as described by Monaghan *et al.* (19). Frozen cells were transferred into a freeze substitution unit (FS 7500, Boeckeler Instruments, Tucson, AZ) precooled to −88 °C for substitution with acetone and subsequent fixation with 0.25% glutaraldehyde and 0.5% osmium tetraoxide at temperatures between −30 °C and +2 °C as described in detail (20) and embedded in Epon. 50–60-nm-thick sections were stained with uranyl-acetate and lead-citrate and analyzed in a transmission electron microscope (CM12; Philips, Eindhoven, The Netherlands) equipped with a CCD camera (Ultrascan 1000; Gatan, Pleasanton, CA) at an acceleration voltage of 100 kV.

Cell Viability Following Cholesterol Loading—Host cells were loaded with cyclodextrin-cholesterol complexes (Sigma) for 24 h at the concentrations indicated in the figure legend, washed in medium, and incubated at 37 °C for additional 24 h. Cell viability was tested by using the AlamarBlue® assay (BIOSOURCE, Camarillo, CA), according to the manufacturer's instructions.

P-glycoprotein Functional Assay—P-gp activity was assessed by cellular retention of the P-gp substrate rhodamine 123 (Rho). Briefly, the cells were incubated with 0.5 μg/ml Rho in PBS for 30 min at 37 °C, washed in PBS, and incubated in medium at 37 °C for the time points indicated in the figure legend. The kinetic of rhodamine retention was quantified by flow cytometry.

Western Blot Analysis—Cell lysates for immunoblots were prepared by sonicating cells at 10^7/ml in 50 mM Tris-HCl (pH 6.8), 10% glycerol, 2% SDS, 5 mM dithiothreitol, 0.5 mM phenylmethylsulfonyl fluoride, and complete protease inhibitor mixture (Calbiochem). Samples corresponding to 40 μg proteins were mixed with SDS-PAGE loading buffer and incubated 10 min at room temperature to prevent P-gp aggregation. The samples were separated on 7.5% SDS-PAGE gels, transferred to nitrocellulose membranes, and probed using anti-P-gp C219 (1:50) and anti-tubulin (1:2000) monoclonal antibodies. Immunoreactive bands were visualized with horseradish peroxidase-conjugated secondary antibodies and ECL.

Determination of Protein Concentration—Protein content was determined using the Bio-Rad Protein Assay according to the instructions provided by the manufacturer. Bovine serum albumin was used for the standard curve.

Statistical Analyses—The data are expressed as the means ± S.E. One-way analysis of variance was performed (GraphPad Prism 4.0c; GraphPad Software, Inc.), and a probability value < 0.05 was considered statistically significant. When the overall probability value was < 0.05, the Dunnett multiple-comparisons test was used as a post-test to determine whether there was a significant difference between values of control (reference sample) and samples of interest.

RESULTS

Host Cell P-gp Is Essential for Normal Parasite Replication—To determine whether the activity of host P-gp plays a role in parasite replication, host cells expressing different levels of the protein (supplemental Fig. S1) were infected with *T. gondii* expressing β-galactosidase, which allows parasite quantification by colorimetric reaction (21). Direct parasite count at 24 h post-infection (p.i.) revealed the presence of smaller vacuoles containing fewer parasites in P-gp-deficient host cells (Fig. 1*A*). Importantly, complementation of P-gp-deficient cells with the human P-gp homologue fully restored parasite replication. Analysis of parasite burden by visualization of parasite vacuoles at 48 h p.i. (Fig. 1*B*) and colorimetric reaction at 48 and 72 h p.i. (Fig. 1*C*) confirmed that *T. gondii* replication was strongly inhibited in the absence of host P-gp. In addition, P-gp-complemented host cells generated a higher *T. gondii* burden than that found in WT cells. To further confirm that P-gp activity confers a replication advantage for the parasite, we used WT 3T3 fibroblasts transfected to overexpress P-gp as host cells (12). Parasite quantification was performed either at the level of single host cells using flow cytometry or as parasite burden of the whole host cell monolayer by colorimetric reaction (supplemental Fig. S2). Both analyses indicated a positive correlation between P-gp expression levels and parasite replication. Absence of the multidrug transporter MRP1, in addition to the two P-gp isoforms (triple KO cells) (11), did not further

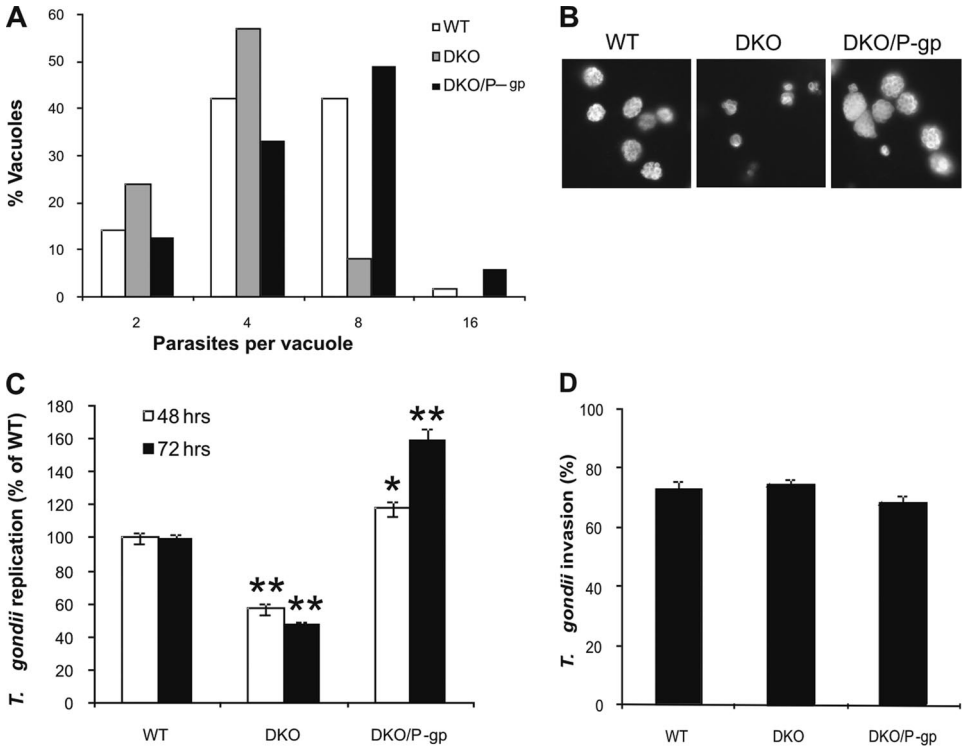

FIGURE 1. **Host cell P-gp modulates parasite replication.** *A*, WT, P-gp-deficient (DKO) and P-gp-complemented (DKO/P-gp) host cells were infected with *T. gondii* at multiplicity of infection 1. After 24 h p.i., intracellular parasites were quantified by direct counting. The distribution of the parasite number in single vacuoles is expressed as percentage of total vacuoles examined ($n > 30$). *B*, immunofluorescence analysis of intracellular vacuoles containing parasites at 48 h p.i. using anti-*T. gondii* serum, followed by fluorescein-conjugated secondary antibodies. *C*, quantification of parasite burden at 48 and 72 h p.i. by a colorimetric assay measuring the amount of parasite-expressed β-galactosidase. The results are expressed as percentages of parasite number in WT host cells ± S.E. ($n = 6$). *, $p < 0.05$; **, $p < 0.01$. *D*, host cell monolayers were incubated with *T. gondii* at a multiplicity of infection of 1. After 2 h of incubation, 20 fields of infected cells were examined, and the number of intracellular invaded parasites was determined as described under "Experimental Procedures." The data are expressed as percentages of total parasite number ± S.E. ($n = 20$).

decrease parasite replication (data not shown). Collectively, these data unambiguously show that the presence of an active P-gp in the host is directly involved in a process controlling *T. gondii* replication.

Host Cell P-gp Is Not Involved in Parasite Invasion—The reduction in parasite number seen in P-gp-deficient cells could have resulted from either decreased parasite replication or decreased invasion efficiency. To assess whether the absence of P-gp on the host plasma membrane compromises the ability of *T. gondii* to enter host cells, an invasion assay was performed using parasites harvested from WT host cells and allowed to infect cells expressing different levels of P-gp. The number of intracellular parasites was comparable in all tested cell lines at 2 h post-infection (Fig. 1*D*), indicating that host P-gp is not required for parasite invasion and that the reduced parasite burden observed in DKO cells is not due to a defect in host cell entry.

Host Cell P-gp Deficiency Inhibits Cholesterol Transport to T. gondii—The reduced parasite replication observed in P-gp-deficient host cells led us to hypothesize that the absence of P-gp may disturb the supply of lipid components necessary for assembly of new parasite membranes. To test this hypothesis, we evaluated cholesterol trafficking and metabolism in the parasite, because *T. gondii* is auxotrophic for cholesterol and depends solely on the host for its supply (22). When we tested the transport of exogenous radiolabeled cholesterol to the parasite, we found that in the absence of host P-gp, cholesterol delivery was strongly reduced (Fig. 2*A*). Importantly, P-gp DKO cells showed normal uptake of exogenous cholesterol (supplemental Fig. S3), indicating that the reduced cholesterol transport to the parasite is not caused by a compromised uptake of this lipid by the host cells. In addition, the increased *T. gondii* replication in P-gp-complemented host cells coincided with enhanced cholesterol delivery to the parasites, suggesting that the level of cholesterol transport was regulating parasite replication rate.

In addition, we monitored the cholesterol transport *in vivo* by using the fluorescently labeled analogue NBD-cholesterol (Fig. 2*B*). Similar to the observations during the radiolabeled cholesterol incubation, transport of NBD-cholesterol to parasites grown in DKO cells was reduced compared with WT cells and a pattern of punctuated structures, reminiscent of endocytic vesicles, accumulated around the parasite vacuoles. Conversely, parasites infecting P-gp-complemented cells showed high level of fluorescence, indicating a robust trafficking of cholesterol to the vacuole.

To test whether decreased cholesterol availability in the absence of host P-gp was directly responsible for the reduced *T. gondii* replication, we evaluated the parasite burden in DKO cells loaded with exogenous cholesterol following infection. This treatment improved parasite replication in a dose-dependent manner (Fig. 2*C*), confirming that insufficient cholesterol availability was indeed the limiting factor for parasite replication.

To investigate the mechanism of P-gp involvement in the cholesterol trafficking to *T. gondii*, we inhibited the vesicular transport of host cholesterol from lysosomes to both plasma membrane and endoplasmic reticulum with the class 2 amphiphile U-18666A (23). Treatment with U-18666A has been shown to decrease the cholesterol delivery to intracellular parasites (22). This broad inhibition of cholesterol trafficking severely affected *T. gondii* replication in WT host cells, with higher levels of inhibition than the ones observed in P-gp defective cells (Fig. 2*D*). On the other hand, parasite replication in DKO cells was further inhibited by only 10% upon U-18666A treatment. The absence of a significant cumulative effect between the lack of P-gp and inhibitor treatment indicates that P-gp may operate, directly or indirectly, on a similar pathway of cholesterol trafficking that is essential for parasite replication.

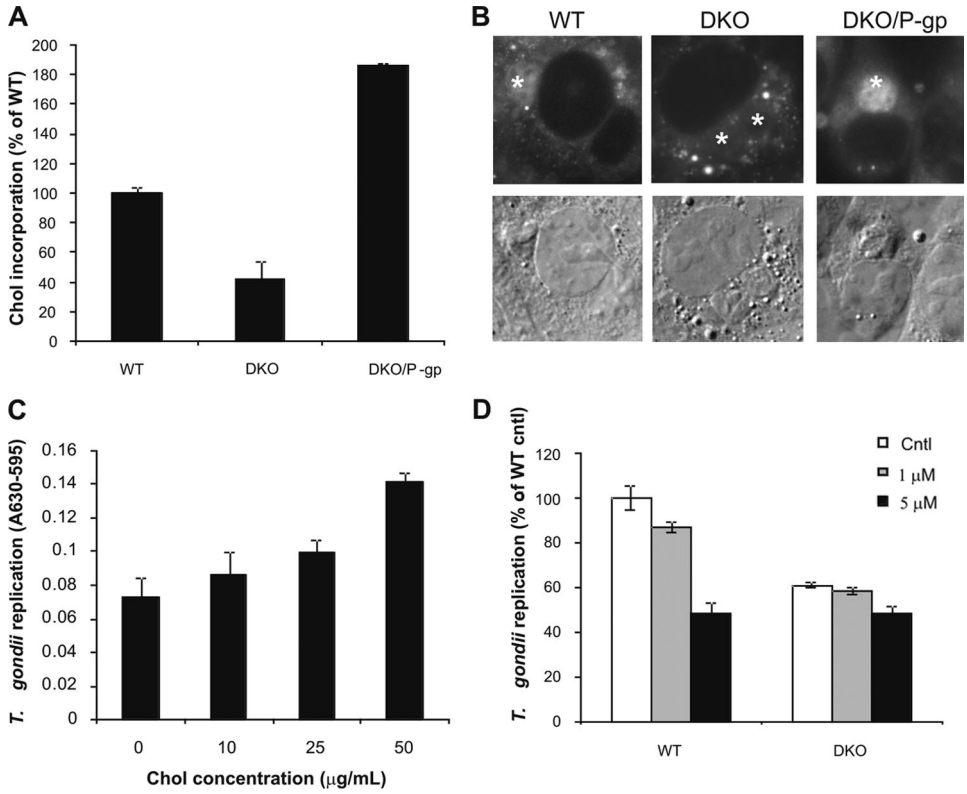

FIGURE 2. **Host cell P-gp deficiency inhibits cholesterol transport to *T. gondii*.** *A*, *T. gondii*-infected host cells were labeled for 5 h with 0.5 μCi/ml [^{3}H]cholesterol. The parasites were isolated, and [^{3}H]cholesterol incorporation was measured by liquid scintillation. The data are expressed as percentages of cholesterol in parasites (dpm/10^6 parasites) isolated from WT host cells $\pm$ S.E. ($n = 6$). *B*, host cell monolayers were infected with *T. gondii* for 24 h followed by incubation with NBD-cholesterol and observed by fluorescence microscopy. The *asterisks* indicate parasite vacuoles. *C*, after *T. gondii* invasion, DKO host cells were loaded with the indicated concentrations of cyclodextrin-cholesterol complexes, and parasite replication was monitored at 48 h p.i. as described in the legend to Fig. 1. The data are averages $\pm$ S.E. ($n = 3$). *D*, after *T. gondii* infection, WT and DKO host cells were treated with the class 2 amphiphile U-18666A at the indicated concentrations, and parasite replication was quantified at 48 h p.i. The results are expressed as percentages of parasite number in untreated (*Cntl*) WT cells. The data are averages $\pm$ S.E. ($n = 6$).

P-gp Associates with the Parasite Vacuole—Our previous results suggest that P-gp may be involved in the cholesterol trafficking to the parasite via the endocytic pathway. To investigate this possibility, we localized host P-gp in infected cells. P-gp is mainly present in the plasma membrane of the cells, but a minority also localizes in intracellular compartments, including endo-lysosomes (24, 25). Because endo-lysosomes have been shown to be recruited to the PV in *T. gondii* infected cells (8), we reasoned that P-gp also associates with the parasite vacuole. To test this hypothesis, we infected P-gp-complemented host cells, whose level of P-gp expression allows analysis by immunofluorescence using the P-gp specific monoclonal antibody C219 (supplemental Fig. S1). This analysis showed that P-gp was predominantly present on the host plasma membrane as expected. In addition, P-gp was also found closely associated with the PV (Fig. 3, *A* and *B*).

Host Organelles Are Recruited to the PV in the Absence of Host P-gp—*T. gondii* scavenges cholesterol from host endo-lysosomal compartments (22), and these organelles are actively recruited by the parasite to the PV in a time-dependent manner after infection (8). To test whether the decreased cholesterol delivery to the parasite in P-gp-deficient cells was due to a failure in recruiting the cholesterol rich endo-lysosomes, we probed the localization of these organelles in infected cells (Fig. 3*C*). First we analyzed the labeling of endocytic vesicles using cholera toxin B-subunit, which binds to the raft-associated sphingolipid GM1 and enters the cell by retrograde transport in the secretory pathway (26). Cholera toxin-positive structures were equally found around the PV of parasites infecting WT, DKO, and P-gp-complemented host cells. Moreover, Lamp1 (lysosome-associated membrane protein 1) staining further confirmed that lysosomes are recruited to the PV in DKO cells. Finally, host Golgi, which was previously shown to redistribute at the PV (8), was also found close to the PV surface in all tested cell lines. Collectively, our results show that the absence of host P-gp does not inhibit the parasite-mediated recruitment of host organelles to the PV.

Cholesterol Accumulates outside the PV in the Absence of Host P-gp—Despite the normal recruitment of lysosomes around the PV in DKO host cells, the accumulation of NBD-cholesterol observed in this cell type (Fig. 2*B*) prompted us to analyze whether the intracellular distribution of endogenous cholesterol is altered in absence of host P-gp. Staining of unesterified cholesterol with the poliene antibiotic filipin (27) in infected WT cells showed labeling of parasite membranes and perinuclear vesicular structures, previously reported to be endo-lysosomal compartments (Fig. 4*A*). On the contrary, in DKO cells the filipin-positive vesicular structures were bigger and more intensely labeled and accumulated outside the PV. Importantly, P-gp complementation prevented the cholesterol accumulation, indicating that the cholesterol accumulation is P-gp-dependent.

Inhibition of Cholesterol Transport to the Parasite Vacuole Does Not Depend on H.O.S.T. Formation—Next we assessed whether the defective transport of cholesterol to the parasite resulted from a faulty formation of the H.O.S.T. system, a recently described structure that can supply the parasite with cholesterol contained in host endo-lysosomes (8). Analysis by electron microscopy found normal recruitment of host organelles to the PV, including mitochondria, both in WT and DKO host cells (Fig. 4*B*, *arrowheads*). Importantly, parasites grown in DKO host cells were able to form H.O.S.T. structures with clearly visible tubules and vesicles (Fig. 4*B*, *arrows* and *magnified images*). Thus, host P-gp is not required for the formation of structurally normal parasite vacuoles. In this respect, the observed inhibition of cholesterol transport despite the for-

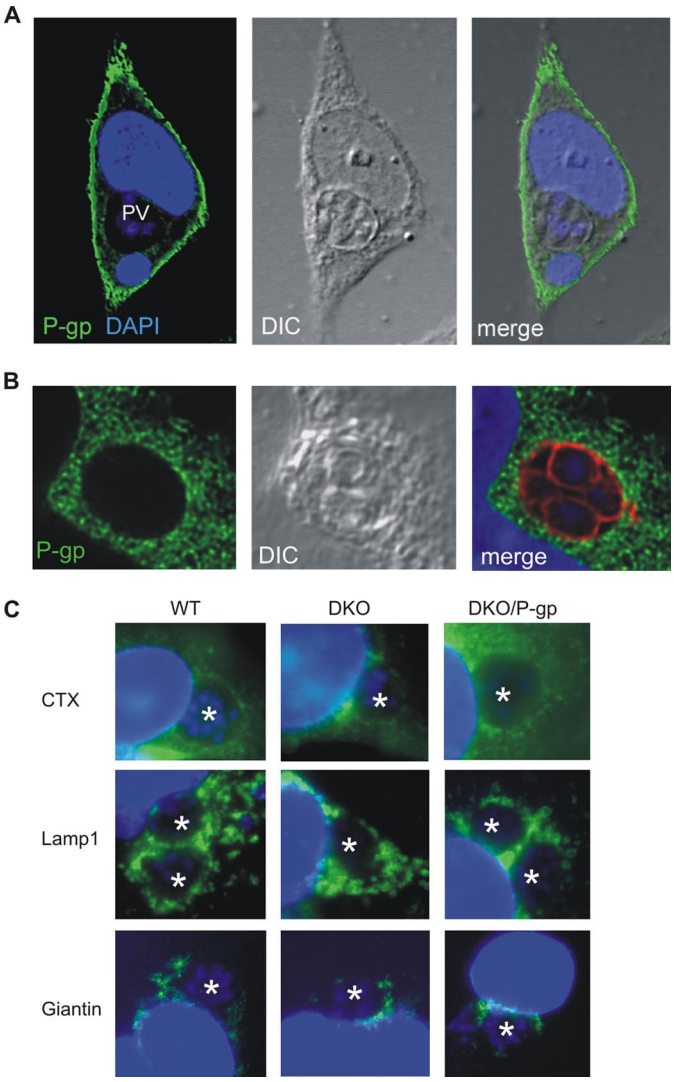

FIGURE 3. **Host P-gp associates with the parasite vacuole.** *A*, confocal microscopy of P-gp localization in P-gp-complemented (DKO/Pgp) cells infected for 24 h with *T. gondii*. Nuclear DNA was stained with 4′,6-diamidino-2-phenylindole (*DAPI*). PV, parasitophorous vacuole. *DIC*, differential interference contrast image. *B*, confocal microscopy of infected cells as described for *A*, showing P-gp (*green*) and parasite (*red*) staining. *C*, fluorescence microscopy of infected WT, P-gp-deficient (DKO) and P-gp-complemented (DKO/P-gp) host cells showing that *T. gondii* PV associated with labeled host endo-lysosomes (cholera toxin (*CTX*)), lysosomes (Lamp1), and Golgi (giantin). The *asterisks* indicate parasite vacuoles.

mation of H.O.S.T. suggests that either P-gp acts at a later stage than the development of these structures, or it affects a H.O.S.T.-independent mechanism of cholesterol delivery. To test the latter hypothesis, we analyzed the replication of *N. caninum*, an apicomplexan parasite related to *T. gondii* whose intracellular vacuoles recruit host endo-lysosomes (supplemental Fig. S4) but are devoid of H.O.S.T (8). As with *T. gondii*, *N. caninum* replication was inhibited in absence of host P-gp and could be rescued by P-gp complementation (Fig. 4*C*). In addition, *N. caninum* growth in DKO host cells resulted in decreased free cholesterol content and cholesteryl ester storage in lipid droplets (Fig. 4*D*), suggesting that P-gp-mediated cholesterol supply to the parasite operates via a mechanism independent of the H.O.S.T. system found in the PV.

Host Cell P-gp Deficiency Affects T. gondii Sphingolipid Metabolism—Our previous results showed that cholesterol transport to the parasite is defective in P-gp-deficient host cells. We then investigated whether this impaired transport affected the lipid content of the parasite. Lipid analyses of *T. gondii* maintained in DKO host cells revealed that the steady state of cholesterol content was comparable with WT after one lysis passage (23 ± 1.6 μg/mg protein) but decreased after prolonged growth in these cells (four lysis passages) (Fig. 5*A*). Similar to the observations in *N. caninum*, a marked decrease in cholesteryl esters stored in lipid droplets was observed in parasites isolated from DKO cells (supplemental Fig. S5).

Because cholesterol is an important regulator of membrane fluidity, membrane domains and signaling processes (reviewed in Ref. 28), we investigated whether the reduced cholesterol content observed in *T. gondii* grown in DKO host cells affected the lipid profile of the parasite membranes. Unexpectedly, liquid chromatography-mass spectrometry analysis of parasite sphingolipids revealed a considerably higher amount of ceramide, ceramide phosphatidylethanolamine, sphingomyelin, and lactosylceramide, whereas the levels of glucosylceramide did not change (Fig. 5*B*). Given the crucial role of ceramide in cell physiology both as a precursor of complex sphingolipids and as a second messenger regulating a variety of cellular processes (reviewed in Ref. 29), we analyzed whether neosynthesis of this lipid was up-regulated in *T. gondii* grown in DKO host cells. Metabolic labeling of extracellular parasites revealed that ceramide synthesis was higher in *T. gondii* isolated from DKO host cells after four lysis passages than in WT cells (Fig. 5*C*), supporting the hypothesis that the higher ceramide levels observed are indeed an active response of the parasite. These results suggest that reduced cholesterol availability triggers compensatory mechanisms in *T. gondii*, presumably to adapt to the intracellular environment of DKO cells and/or to adjust the lipid composition of its membranes.

Absence of P-gp Alters Normal Cholesterol Metabolism in Uninfected Fibroblasts—The observed inhibition of cholesterol transport to the parasite and the accumulation of cholesterol-loaded organelles around the PV in P-gp-deficient host cells prompted us to analyze whether P-gp is also involved in cholesterol trafficking in uninfected host cells. To test this hypothesis, we investigated whether P-gp expression levels correlated with alterations in cholesterol metabolism in fibroblasts. Analysis of intracellular cholesterol distribution visualized with filipin revealed that P-gp DKO cells accumulated cholesterol in perinuclear vesicles compared with WT and P-gp-complemented cells (Fig. 6*A*). In addition, despite comparable uptake of radiolabeled cholesterol (supplemental Fig. S3), DKO cells showed a time-dependent increase in cholesterol esterification compared with WT cells (Fig. 6*B*). On the other hand, P-gp complementation of DKO cells lowered the levels of cholesterol esterification. This correlation between the absence of P-gp and increased cholesterol esterification was evident not only in the kinetics of the process, but also in the steady state cholesteryl ester content (supplemental Fig. S6). Next we evaluated cholesterol levels in the plasma membrane by extraction with CD or efflux to the extracellular acceptors

reconstituted HDL (30) and apoA-I. We found that less cholesterol could be extracted with CD from the plasma membrane of DKO cells and that P-gp complementation increased the level of cholesterol extraction (Fig. 6*C*). Furthermore, P-gp complementation also enhanced the ABCA1-mediated efflux of cholesterol to its natural acceptor HDL (Fig. 6*D*) and apoA-I (Fig. 6*E*). These data reveal that cells deficient in P-gp accumulated free and esterified cholesterol in perinuclear vesicular structures and cytosolic lipid droplets, respectively. On the other hand, cells expressing high levels of P-gp showed increased amounts of cholesterol in the plasma membrane, which then resulted in increased efflux to extracellular acceptors. To further test whether WT cells were more prone to accumulate free cholesterol in the plasma membrane than DKO cells, we exploited the toxicity induced by destabilizing the plasma membrane via exogenous cholesterol loading. Analysis of cell viability showed that DKO cells were minimally affected by exogenous cholesterol loading, whereas viability decreased with increasing levels of P-gp expression in WT and P-gp-complemented cells (Fig. 6*F*). As previously reported in cholesterol-loaded macrophages (31), blocking cholesterol transport from lysosomes to the plasma membrane using the hydrophobic amine U-18666A (23) prevented the cholesterol toxicity in P-gp-expressing cells but did not alter the viability of DKO cells (data not shown). Thus, these data suggest that inhibition of intracellular cholesterol transport mimics the increased survival of DKO cells during cholesterol loading.

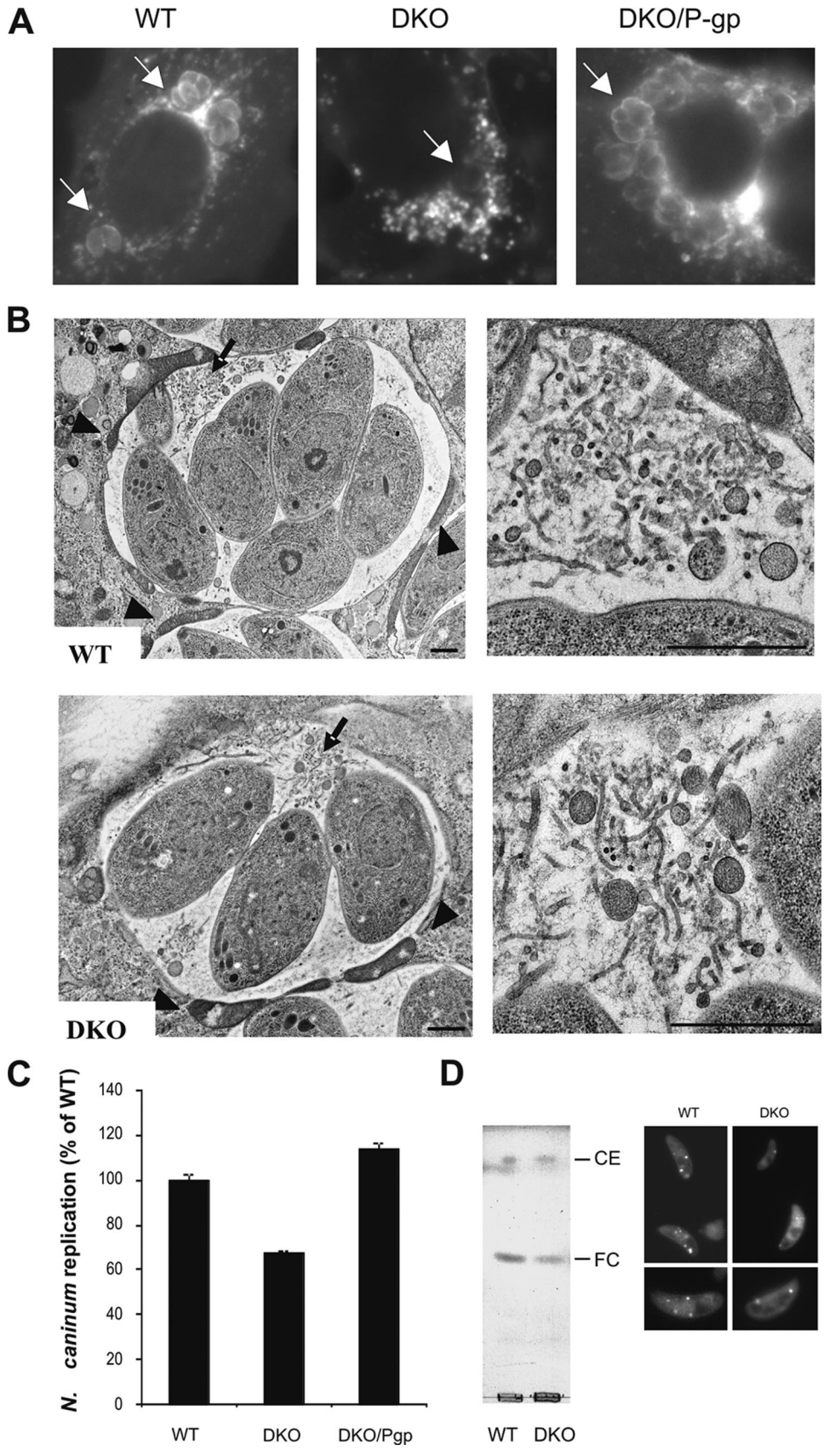

DISCUSSION

P-gp is a unique transporter because of its broad substrate specificity, and its expression constitutes a major obstacle in the fight against multidrug-resistant tumor cells and pathogens. Yet P-gp also plays a key

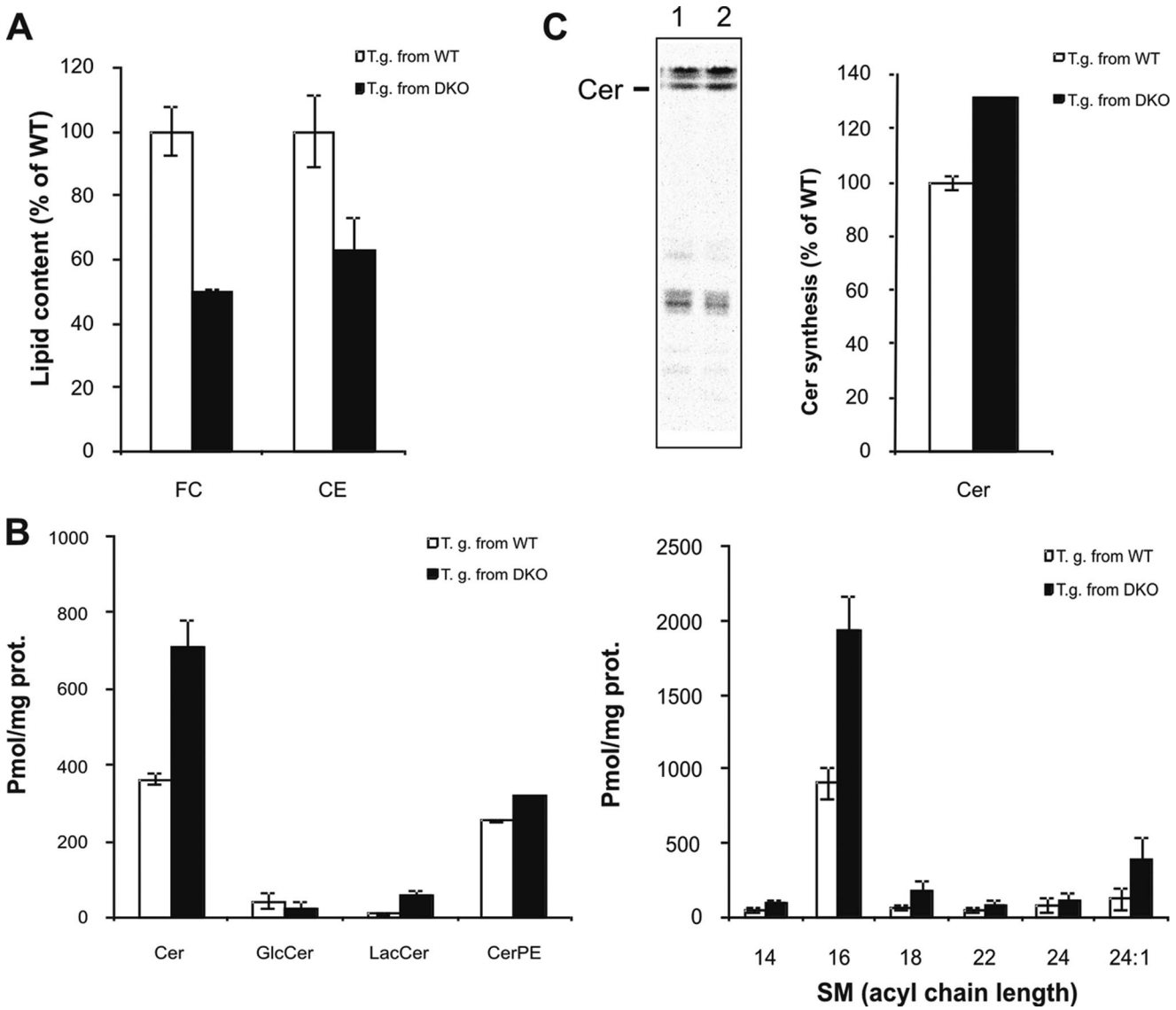

FIGURE 5. **Host cell P-gp deficiency affects *T. gondii* lipid metabolism.** *A*, quantification of free cholesterol (*FC*) and cholesteryl esters (*CE*) by enzymatic reaction (Amplex red®) in *T. gondii* isolated from WT or DKO host cells after four lysis passages. The data are expressed as percentages of lipid content in *T. gondii* from WT cells ± S.E. ($n = 5$). *B*, liquid chromatography-mass spectrometry analysis of sphingolipids of *T. gondii* isolated from WT or DKO host cells after four lysis passages. The data are averages ± S.E. ($n = 3$) of a representative from two experiments done in triplicate. *Cer*, ceramide; *GlcCer*, glucosylceramide; *LacCer*, lactosylceramide; *CerPE*, ceramide phosphoethanolamine. The predominantly detected C16 species are plotted. *SM*, sphingomyelin. *C*, *left panel*, TLC separation of *de novo* synthesized lipids labeled with [^{3}H]palmitic acid in *T. gondii* isolated from WT (1) or DKO (2) cells. *Right panel*, newly synthesized ceramide is expressed as a percentage of ceramide in *T. gondii* isolated from WT host cells. The data are averages ± S.E. ($n = 3$).

role in normal physiological processes, including preventing cellular toxicity at the blood brain barrier, as shown *in vivo* by the extremely high sensitivity of P-gp KO mice to toxic compounds (32).

Our aim was to investigate whether host P-gp plays a role in host-pathogen interaction that is distinct from multidrug resistance. Previous studies using P-gp inhibitors suggested that *T. gondii* may require a functional P-gp to survive in the host cell (33). In the present work more detailed investigation found that host P-gp is in fact a crucial modulator of *T. gondii* and *N. caninum* replication. In addition, we found that host P-gp is not a receptor for the parasite, and its absence does not affect parasite invasion or the formation of structurally normal parasite vacuoles. Importantly, we found that transport of cholesterol from the host cell to the parasites, a process on which *T. gondii* is completely dependent, was impaired in absence of

FIGURE 4. **Cholesterol accumulates outside the parasite vacuole in absence of host P-gp.** *A*, WT, P-gp-deficient (DKO), and P-gp-complemented (DKO/P-gp) host cell monolayers were infected with *T. gondii* for 24 h. After fixation, the intracellular distribution of unesterified cholesterol was visualized with filipin and observed by fluorescence microscopy. The *arrows* indicate parasite vacuoles. *B*, electron microscopy of *T. gondii* infected WT and P-gp-deficient (DKO) host cells at 24 h p.i., showing PV-associated mitochondria (*arrowheads*) and H.O.S.T. structures (*arrows*). *Right panels*, magnification of H.O.S.T. structures. *Scale bars*, 2 μm. *C*, host cells monolayers were infected with *N. caninum* and parasite replication quantified at 72 h p.i., as described. The results are expressed as percentages of parasite number in WT host cells ± S.E. ($n = 3$). *D*, lipids were extracted from *N. caninum* isolated from WT or DKO host cells after four lysis passages. A representative TLC of lipids corresponding to equal protein amount is shown. Free cholesterol (*FC*) and cholesteryl esters (*CE*) were visualized with $CuSO_4$. *Inset*, Nile red staining of cholesteryl esters-containing lipid droplets in parasites isolated from WT or DKO host cells after four lysis passages.

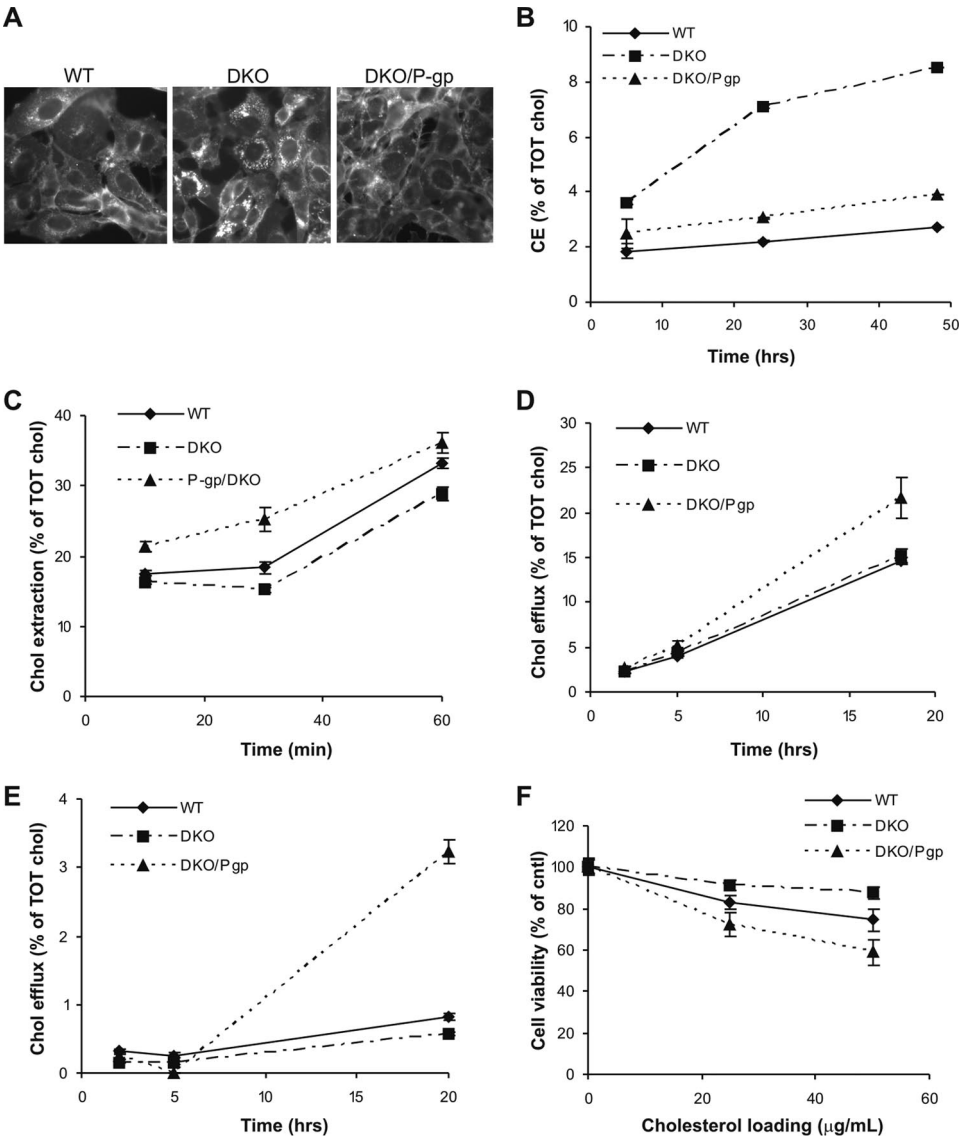

FIGURE 6. **P-gp expression alters cholesterol metabolism in fibroblasts.** *A*, filipin labeling of WT, P-gp-deficient (DKO), and P-gp-complemented (DKO/P-gp) host cells monolayers to visualize the intracellular distribution of unesterified cholesterol. *B*, host cells were labeled with [^{3}H]cholesterol, and the time course of [^{3}H]cholesterol esterification was measured at the indicated time points. The data are percentages of [^{3}H]cholesteryl esters (*CE*) of total cellular [^{3}H]cholesterol. *C*, cells were labeled with [^{3}H]cholesterol for 24 h, washed, and incubated with 2 mM methyl-β-cyclodextrin. Medium aliquots were taken at the indicated time points, and extracted [^{3}H]cholesterol was measured by liquid scintillation. Extracted cholesterol is expressed as a percentage of total [^{3}H]cholesterol (medium + cell associated radioactivity). *D* and *E*, the cells were similarly labeled and incubated with 20 μg/ml reconstituted HDL (*D*) or 10 μg/ml apoA-I (*E*). Cholesterol efflux is expressed as a percentage of total [^{3}H]cholesterol as before. *F*, cells were loaded with the indicated concentrations of cyclodextrin-cholesterol complexes for 24 h, and viability was measured by AlamarBlue® assay. Results are expressed as percentage of untreated (*cntl*) cell viability. All of the data are averages ± S.E. ($n = 3$).

host P-gp. Biochemical analyses revealed that the lipid composition of the parasite was altered when grown in P-gp-deficient host cells. Specifically, both free and esterified cholesterol levels were reduced, as expected from a decreased uptake of cholesterol from the host; interestingly, the content of selected sphingolipids also changed compared with *T. gondii* grown in WT cells. In particular, the level of sphingomyelin, a major structural sphingolipid mainly found on the plasma membrane, was increased 2-fold. Sphingomyelin has a high affinity for and closely associates with cholesterol and both lipids contribute to the ordered state of plasma membrane domains. Although it is well accepted that cholesterol homeostasis is modulated by sphingomyelin content, studies on the regulation of sphingomyelin metabolism by varying the cellular cholesterol levels produced contradictory results in different cell types analyzed (reviewed in Ref. 34). However, cholesterol depletion was shown to stimulate sphingomyelin synthesis in fibroblasts (35), and high levels of sphingolipids can retain the ordered state of model membranes (36), suggesting that in conditions of cholesterol depletion, increased sphingomyelin content could still contribute to the maintenance of an ordered plasma membrane structure. Thus, it is possible that the increased sphingomyelin content detected in parasites with limited cholesterol levels plays a role in conserving the structural properties of parasite membranes.

Also noteworthy was the increased ceramide content in parasites from P-gp-deficient host cells. It is tempting to speculate that this elevation is a compensatory mechanism for the decreased cholesterol in the membranes, because ceramide-cholesterol replacement has been shown to occur *in vitro* (37). However, the ceramide increase observed does not justify this hypothesis, because similarly for mammalian cells, ceramide in the parasite is about 10 times less abundant than cholesterol. On the other hand, ceramide plays a well known role of second messenger in a variety of cellular processes, including stress response (reviewed in Ref. 38); thus it seems more likely that the enlarged ceramide pool helps to fulfill the signaling needs of *T. gondii* in a host cell environment not optimal for parasite survival. The increased ceramide synthesis observed in labeled parasites isolated from P-gp-deficient host cells supports the idea that the content of this lipid is modulated at least in part by an active synthetic process in the parasite. Scavenging of sphingolipids from the host cell cannot be excluded at this stage, although it has not been demonstrated to date in this parasite.

Although our results clearly indicate that cholesterol transport from the host to the parasite is defective in absence of host P-gp, the data regarding the modality of this transport were quite surprising. So far, *T. gondii* has been shown to depend on

two forms of host-derived cholesterol: free cholesterol contained in endo-lysosomes (22) and esterified cholesterol present in cytosolic lipid bodies (14). The former requires functional host vesicular trafficking (22, 39) and relies on the recruitment of host endo-lysosomes around the PV and their diversion to the PV interior via the formation of H.O.S.T. structures (8). Our data show that P-gp-deficient cells were competent for cholesterol esterification, endo-lysosome recruitment to the PV, and H.O.S.T. formation; thus, the inhibition of cholesterol trafficking to the parasite cannot be attributed to lack of these processes. However, the observed accumulation of cholesterol in endo-lysosomes in P-gp-deficient cells raised the possibility that P-gp contributes to the cholesterol mobilization from lysosomes, a crucial process for cholesterol trafficking to the PV (8, 22). Thus, P-gp in endocytic compartments (25) could help to mobilize cholesterol from endo-lysosomes either juxtaposed to or internalized in the PV via the H.O.S.T. system. This scenario is also in agreement with the reduced cholesterol content in *N. caninum* when grown in P-gp-deficient cells, because the PV of this parasite does not contain H.O.S.T. but is in close proximity with host endo-lysosomes.

Collectively, these results show that host P-gp plays an important role in cholesterol transport to the parasite vacuole. However, there are several observations implying that P-gp does not control all cholesterol transport to the parasite and that P-gp-independent transport pathways must also exist, namely (i) the slight (10%) additional inhibition of parasite replication in DKO cells following U-18666A drug treatment, (ii) the increased parasite replication upon cholesterol loading of DKO cells, and (iii) the ability of the parasite to replicate in DKO cells for several lysis passages.

Considering these results, it seems that the mechanism underlying P-gp-mediated cholesterol transport to the parasite is most likely to fall within one of two general scenarios, namely (i) P-gp does not transport cholesterol directly but is critical in another yet unidentified cellular process essential for cholesterol transport and parasite replication or (ii) P-gp plays a direct but seemingly not exclusive role in cholesterol transport and/or metabolism. The role of P-gp as a transporter of cellular cholesterol has been the subject of considerable debate. Although the presence of cholesterol in the membrane surrounding P-gp is crucial for the ATPase activity of the protein (40), results of studies addressing the role of P-gp in cholesterol trafficking have been contradictory. P-gp has been proposed to translocate cholesterol between the plasma membrane leaflets *in vitro* (40). In addition, several reports using chemically selected cell lines or inhibitors associated P-gp overexpression with increased cholesterol transport to the endoplasmic reticulum and consequent esterification (reviewed in Ref. 41). However, from these studies it is not clear whether the enhanced cholesterol trafficking observed is due to a direct role of the protein or to an elevated turnover of the cholesterol-rich membranes where P-gp is located (42). Our understanding of P-gp-mediated cholesterol transport is further compromised by the contradictory results obtained through the use of P-gp inhibitors with potential side effects and cell type-specific outcome of P-gp expression (41). In our work using P-gp-deficient cells, we found that free cholesterol accumulated in vesicular structures located in the perinuclear region and that this accumulation was absent once P-gp activity was restored. In addition, contrary to previous reports using P-gp inhibitors (43, 44) or selected MDR cell lines (45), cholesteryl esters accumulated in the absence of P-gp. Interestingly, a similar increase in cholesterol esterification was observed *in vivo* in the liver of P-gp-deficient mice (46). Furthermore, we found a positive correlation between cholesterol extractability/efflux from the plasma membrane and P-gp expression. Taken together, our results suggest that P-gp does play a significant role in cholesterol transport in both host-parasite interaction and in normal metabolism of fibroblasts.

Thus, although an indirect effect on cholesterol transport in the absence of P-gp cannot be completely excluded, we observed a number of indications consistent with a model in which P-gp resident in the endo-lysosomes is involved in cholesterol mobilization from these compartments to the PV in case of parasite infection. These indications include: the endo-lysosome recruitment around the PV in infected cells, the cholesterol accumulation outside the PV, the reduced cholesterol supply to the parasite in the absence of host P-gp, and the observation that P-gp-mediated parasite inhibition depends on vesicular trafficking of cholesterol. In addition, several alterations in cholesterol metabolism observed in DKO host cells also suggest that P-gp plays a role in cholesterol trafficking from endo-lysosomes to the plasma membrane in uninfected cells. Such observations include the accumulation of free cholesterol in endo-lysosome like structures in the absence of P-gp, the decreased recycling of exogenous cholesterol to the plasma membrane, and the increase in cholesterol esterification. On the other hand, increased P-gp expression in host cells correlates with increased cholesterol content in the plasma membrane and efflux and increased sensitivity to cholesterol loading toxicity.

In summary, our studies using the intracellular parasites *T. gondii* and *N. caninum* provide evidence that host cell P-gp plays a previously unidentified role in host-parasite interaction. Our results reveal that host P-gp is required for cholesterol transport to the parasite vacuole via a mechanism independent of H.O.S.T. formation and is also involved in normal cholesterol metabolism in uninfected mammalian fibroblasts.

Acknowledgments—We thank Alfred Schinkel for kindly providing the P-gp-deficient murine embryonic fibroblasts, Michael M. Gottesman for the P-gp-complemented murine embryonic fibroblasts and P-gp overexpressing 3T3 fibroblasts, and Peter Lerch for the reconstituted HDL and apolipoprotein A-I. We are grateful to John Boothroyd and David Sibley for the β-galactosidase-expressing T. gondii and N. caninum, to Jack Rohrer and Mohamed-Ali Hakimi for providing anti-giantin and anti-tubulin antibodies, and to Therese Michel and Eva Dalmau for technical assistance. In particular, we thank Piet Borst and Gerrit van Meer for invaluable advice and discussion.

REFERENCES

1. Loo, T. W., and Clarke, D. M. (1999) *Biochem. Cell Biol.* **77,** 11–23
2. Gottesman, M. M., Hrycyna, C. A., Schoenlein, P. V., Germann, U. A., and Pastan, I. (1995) *Annu. Rev. Genet.* **29,** 607–649
3. van Veen, H. W., and Konings, W. N. (1998) *Biochim. Biophys. Acta* **1365,** 31–36

4. Blackmore, C. G., McNaughton, P. A., and van Veen, H. W. (2001) *Mol. Membr. Biol.* **18,** 97–103
5. Maubon, D., Ajzenberg, D., Brenier-Pinchart, M. P., Dardé, M. L., and Pelloux, H. (2008) *Trends Parasitol.* **24,** 299–303
6. Mordue, D. G., Håkansson, S., Niesman, I., and Sibley, L. D. (1999) *Exp. Parasitol.* **92,** 87–99
7. Martin, A. M., Liu, T., Lynn, B. C., and Sinai, A. P. (2007) *J. Eukaryot. Microbiol.* **54,** 25–28
8. Coppens, I., Dunn, J. D., Romano, J. D., Pypaert, M., Zhang, H., Boothroyd, J. C., and Joiner, K. A. (2006) *Cell* **125,** 261–274
9. Schinkel, A. H., Mayer, U., Wagenaar, E., Mol, C. A., van Deemter, L., Smit, J. J., van der Valk, M. A., Voordouw, A. C., Spits, H., van Tellingen, O., Zijlmans, J. M., Fibbe, W. E., and Borst, P. (1997) *Proc. Natl. Acad. Sci. U.S.A.* **94,** 4028–4033
10. Alemán, C., Annereau, J. P., Liang, X. J., Cardarelli, C. O., Taylor, B., Yin, J. J., Aszalos, A., and Gottesman, M. M. (2003) *Cancer Res.* **63,** 3084–3091
11. Wijnholds, J., deLange, E. C., Scheffer, G. L., van den Berg, D. J., Mol, C. A., van der Valk, M., Schinkel, A. H., Scheper, R. J., Breimer, D. D., and Borst, P. (2000) *J. Clin. Invest.* **105,** 279–285
12. Currier, S. J., Kane, S. E., Willingham, M. C., Cardarelli, C. O., Pastan, I., and Gottesman, M. M. (1992) *J. Biol. Chem.* **267,** 25153–25159
13. Hemphill, A., Gottstein, B., and Kaufmann, H. (1996) *Parasitology* **112,** 183–197
14. Sonda, S., Ting, L. M., Novak, S., Kim, K., Maher, J. J., Farese, R. V., Jr., and Ernst, J. D. (2001) *J. Biol. Chem.* **276,** 34434–34440
15. Fuchs, N., Sonda, S., Gottstein, B., and Hemphill, A. (1998) *J. Parasitol.* **84,** 753–758
16. Hemphill, A. (1996) *Infect. Immun.* **64,** 4279–4287
17. Bligh, E. G., and Dyer, W. J. (1959) *Can. J. Med. Sci.* **37,** 911–917
18. Munoz-Olaya, J. M., Matabosch, X., Bedia, C., Egido-Gabás, M., Casas, J., Llebaria, A., Delgado, A., and Fabriàs, G. (2008) *Chem. Med. Chem.* **3,** 946–953
19. Monaghan, P., Cook, H., Hawes, P., Simpson, J., and Tomley, F. (2003) *J. Microsc.* **212,** 62–70
20. Wild, P., Schraner, E. M., Adler, H., and Humbel, B. M. (2001) *Microsc. Res. Tech.* **53,** 313–321
21. McFadden, D. C., Seeber, F., and Boothroyd, J. C. (1997) *Antimicrob. Agents Chemother.* **41,** 1849–1853
22. Coppens, I., Sinai, A. P., and Joiner, K. A. (2000) *J. Cell Biol.* **149,** 167–180
23. Underwood, K. W., Andemariam, B., McWilliams, G. L., and Liscum, L. (1996) *J. Lipid Res.* **37,** 1556–1568
24. Kim, H., Barroso, M., Samanta, R., Greenberger, L., and Sztul, E. (1997) *Am. J. Physiol. Cell Physiol.* **273,** C687–702
25. Fu, D., and Roufogalis, B. D. (2007) *Am. J. Physiol. Cell Physiol.* **292,** C1543–1552
26. Lencer, W. I., and Saslowsky, D. (2005) *Biochim. Biophys. Acta* **1746,** 314–321
27. Zhang, M., Dwyer, N. K., Neufeld, E. B., Love, D. C., Cooney, A., Comly, M., Patel, S., Watari, H., Strauss, J. F., 3rd, Pentchev, P. G., Hanover, J. A., and Blanchette-Mackie, E. J. (2001) *J. Biol. Chem.* **276,** 3417–3425
28. Maxfield, F. R., and Tabas, I. (2005) *Nature* **438,** 612–621
29. Lahiri, S., and Futerman, A. H. (2007) *Cell Mol. Life Sci.* **64,** 2270–2284
30. Lerch, P. G., Förtsch, V., Hodler, G., and Bolli, R. (1996) *Vox Sang* **71,** 155–164
31. Warner, G. J., Stoudt, G., Bamberger, M., Johnson, W. J., and Rothblat, G. H. (1995) *J. Biol. Chem.* **270,** 5772–5778
32. Schinkel, A. H., Smit, J. J., van Tellingen, O., Beijnen, J. H., Wagenaar, E., van Deemter, L., Mol, C. A., van der Valk, M. A., Robanus-Maandag, E. C., te Riele, H. P., Berns, A. J., and Borst, P. (1994) *Cell* **77,** 491–502
33. Silverman, J. A., Hayes, M. L., Luft, B. J., and Joiner, K. A. (1997) *Antimicrob. Agents Chemother.* **41,** 1859–1866
34. Ridgway, N. D. (2000) *Biochim. Biophys. Acta* **1484,** 129–141
35. Leppimäki, P., Kronqvist, R., and Slotte, J. P. (1998) *Biochem. J.* **335,** 285–291
36. Brown, R. E. (1998) *J. Cell Sci.* **111,** 1–9
37. Megha, and London, E. (2004) *J. Biol. Chem.* **279,** 9997–10004
38. Hannun, Y. A., and Obeid, L. M. (2008) *Nat. Rev. Mol. Cell Biol.* **9,** 139–150
39. Sehgal, A., Bettiol, S., Pypaert, M., Wenk, M. R., Kaasch, A., Blader, I. J., Joiner, K. A., and Coppens, I. (2005) *Traffic* **6,** 1125–1141
40. Garrigues, A., Escargueil, A. E., and Orlowski, S. (2002) *Proc. Natl. Acad. Sci. U.S.A.* **99,** 10347–10352
41. Orlowski, S., Martin, S., and Escargueil, A. (2006) *Cell Mol. Life Sci.* **63,** 1038–1059
42. Liscovitch, M., and Lavie, Y. (2000) *Trends Biochem. Sci.* **25,** 530–534
43. Debry, P., Nash, E. A., Neklason, D. W., and Metherall, J. E. (1997) *J. Biol. Chem.* **272,** 1026–1031
44. Luker, G. D., Nilsson, K. R., Covey, D. F., and Piwnica-Worms, D. (1999) *J. Biol. Chem.* **274,** 6979–6991
45. Santini, M. T., Romano, R., Rainaldi, G., Filippini, P., Bravo, E., Porcu, L., Motta, A., Calcabrini, A., Meschini, S., Indovina, P. L., and Arancia, G. (2001) *Biochim. Biophys. Acta* **1531,** 111–131
46. Luker, G. D., Dahlheimer, J. L., Ostlund, R. E., Jr., and Piwnica-Worms, D. (2001) *J. Lipid Res.* **42,** 1389–1394